Angular Distribution of Molecules Sputtered by Gas Cluster Ion Beams and Implications for Secondary Neutral Mass Spectrometry

– Supporting Information –

Matthias Lorenz,[*†] *Alexander G. Shard,*[†] *Jonathan D. P. Counsell,*[‡]

Simon Hutton,[‡] *Ian S. Gilmore*[†]

[†]National Physical Laboratory, Hampton Road, Teddington TW11 0LW, United Kingdom

[‡]Kratos Analytical Ltd., Trafford Wharf Rd, Manchester M17 1GP, United Kingdom

Ejection Probability Distribution

Target material is sputtered by primary ion projectiles and ejecta are captured on a planar surface at distance R in forward direction. The ejecta are assumed to stay within a solid angle 2α while propagating from a point source at the center of the sputter crater. The captured material is spread over an elliptical surface area A' as defined by the intersection of this spherical cone with the planar collector plane at an angle β between the cone height vector and the collector surface normal.

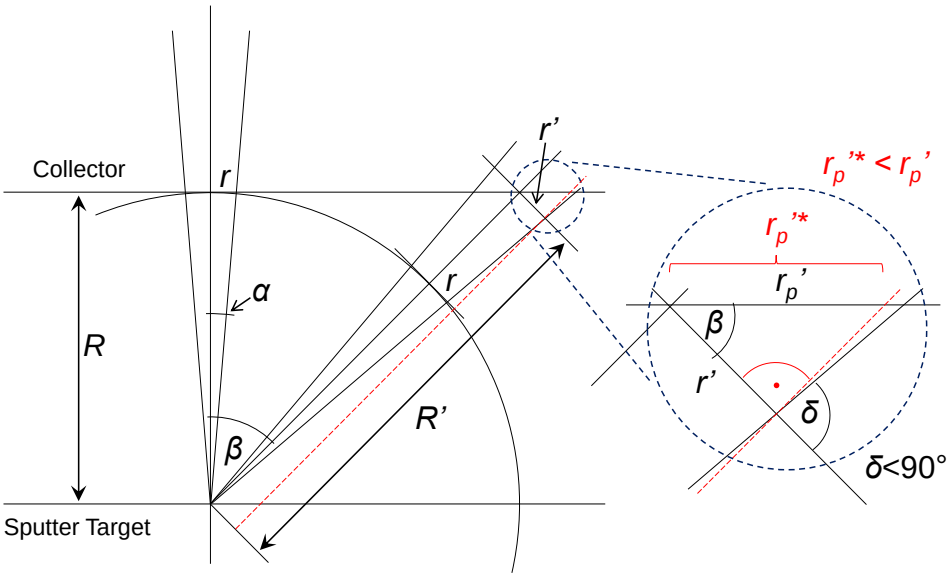

Figure SI-1. Schematic of the sputtering geometry. R – Shortest distance of collector plate from center of sputter crater; R' – Distance from the center of the sputter crater; 2α – Solid angle for ejecta transport from sputter site to collector; β – Angle between planar collector surface normal and distance vector.

Figure SI-1 shows the geometric relations used to derive a correction factor for thickness of the layer of collected material deposited on the collector surface. The spread of ejecta is minimal for the ejecta cone in perpendicular orientation to the collector plane (i.e., cone height equals the

distance between the sputter crater and the collector plane). The cone base surface area on the collector plate is then given by

$$A = \pi r^2 \tag{1}$$

with r defined as

$$r = R \tan \alpha \tag{2}$$

The effective height r' of the ejecta cone increases with the angle β according to eqs 3 and 4

$$r/R = r'/R' \tag{3}$$

$$\cos \beta = R/R' \text{ and } \cos \beta = r/r' \tag{4}$$

Ejecta are spread across an elliptical surface area that is defined by the intersection of the spherical ejecta cone and the planar collector surface at angle β. The surface area can be calculated as

$$A'_p = \pi r' r'_p \tag{5}$$

A cylindrical expansion rather than an ejecta cone shall be assumed in this step (cf. Fig. S1-1) to derive an expression for the surface area in dependence on the average impact angle of the ejecta impinging on the collector surface. It follows eq 6:

$$A'_p \cong A'^*_p = \pi r' r'^*_p \tag{6}$$

Using

$$r'^*_p = r' \cos^{-1} \beta \tag{7}$$

and eq 4, eq 6 can be developed to:

$$A'^*_p = \pi r^2 \cos^{-3} \beta \tag{8}$$

The approximation in eq 6 enables to derive an expression for the change of the collector surface area with the angle β without knowledge of the ejecta cone α:

$$A'_p/A \cong A'^*_p/A = \cos^{-3} \beta \tag{9}$$

A factor $\chi(x,y)$ was introduced to correct the thickness maps ($T(x,y)$ vs. x,y) for the spread of material across an area that increases with angle β. A second correction term $\tau(z,z_0)$ was used to scale absolute thickness values in the maps for the two collector plates used in each experiment in dependence on the minimum distance from the sputter site, z, relative to a common reference distance, z_0. A normalization factor N was introduced to derive eq 10 for the calculation of ejection probability maps $P(x,y)$ from the maps $T(x,y)$ of the deposit thickness values as measured by mapping ellipsometry.

$$P(x,y) = N \cdot \tau(z,z_0) \cdot \chi(x,y) \cdot T(x,y) \qquad (10)$$

with

$$\chi(x,y) = \cos^{-3}\beta(x,y)$$

$$\tau(z,z_0) = (z/z_0)^2$$

The spatial overlap of neighboring spots in the thickness maps was ignored. To minimize the effect of the impact angle dependence of the sticking probability, thickness maps $T(x,y)$ for the organic deposits were confined to areas with $\chi(x,y) \leq 8$, corresponding to a maximum impact angle of ejecta of 60°. Larger gaps in the graphs visible between front (or back) and side collector plates are in part due to the cropping of the thickness maps.

Absolute Thickness Maps for the 15° Angle of Incidence Case

Figure SI-2 shows thickness maps $T(x, y)$ for the organic deposits as captured in a sputtering experiment at 15° polar angle of incidence for the primary ion GCIB. Shown are the absolute thickness maps $T(x, y)$ of the organic deposits as contour lines, rather than maps of the corrected values $P(x, y)$ for the ejection probability.

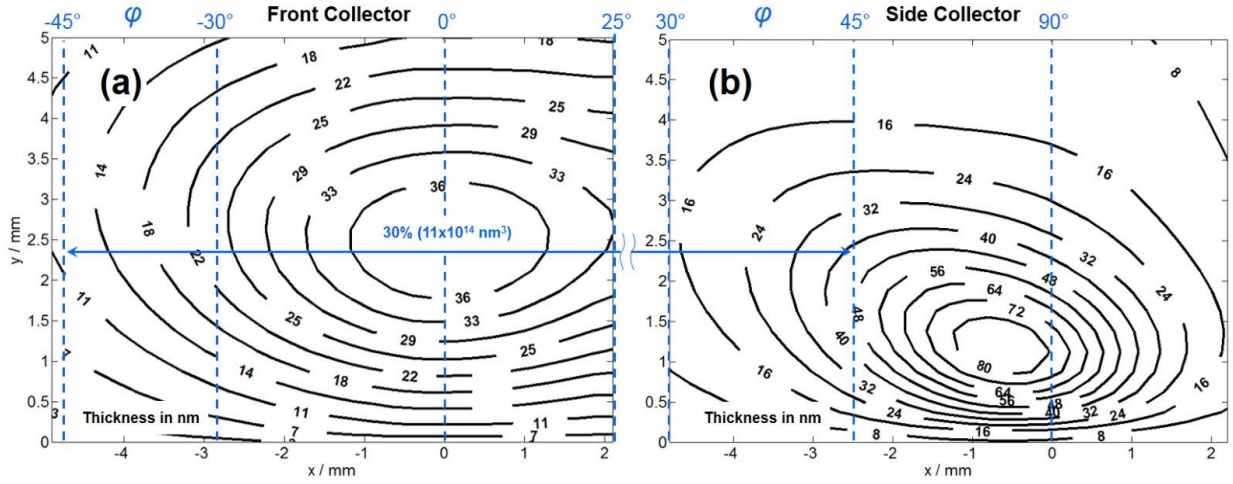

Figure SI-2. Measured thickness maps for deposits collected on the (a) front and (b) side collector during sputtering with E/n = 5 eV 10 keV Ar_{2000} projectiles at 15º. A crater of 1.65 × 1.24 mm^2 surface area was eroded into a ~1.7 µm thick layer of Irganox 1010. The contours are labeled with absolute values for the organic deposit thickness in nm.

Clearly visible in the thickness maps are the pronounced geometrical effects that come with the utilization of planar collector surfaces, convoluted into the raw data. The thickest deposits are usually observed in line with the sputter crater, simply due to the smaller surface area that the material ejected at the corresponding angles is spread across. The information on the angular sputtering distribution is superposed by the more apparent change that goes along with the geometry of sputtering and capturing the ejected material.

Structure and Fragmentation Pathways of Irganox 1010

Figure SI-3 shows the molecular structure of Irganox 1010 with possible positions for fragmentation indicated.

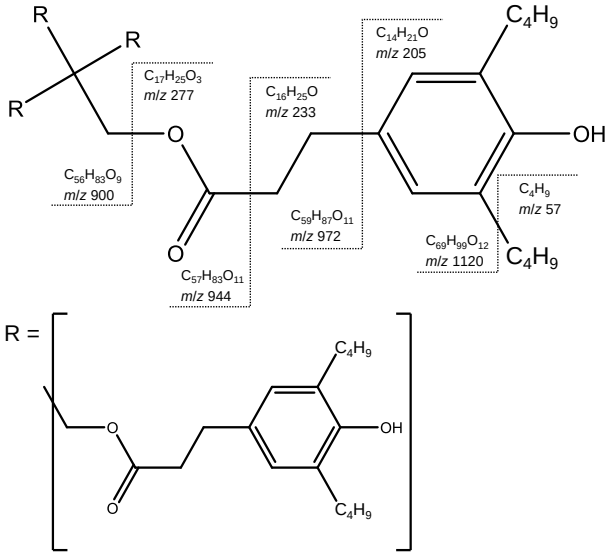

Figure SI-3. Structure and potential fragmentation of the Irganox 1010 molecule ($C_{73}H_{108}O_{12}$, 1176.8 Da).

Angular Dependence of the Chemical Composition of Ejecta

Figure SI-4 shows SIMS spectra recorded for different regions on a front collector plate, thus representing the chemical change of the collected material over a wide range of azimuthal (φ = 0–54º) and polar (θ = 40–82º) angles. The spectra in panels (b) to (e) have been extracted as the average for 500 µm square areas from a single large stage scan experiment. They are thus quantitatively comparable.

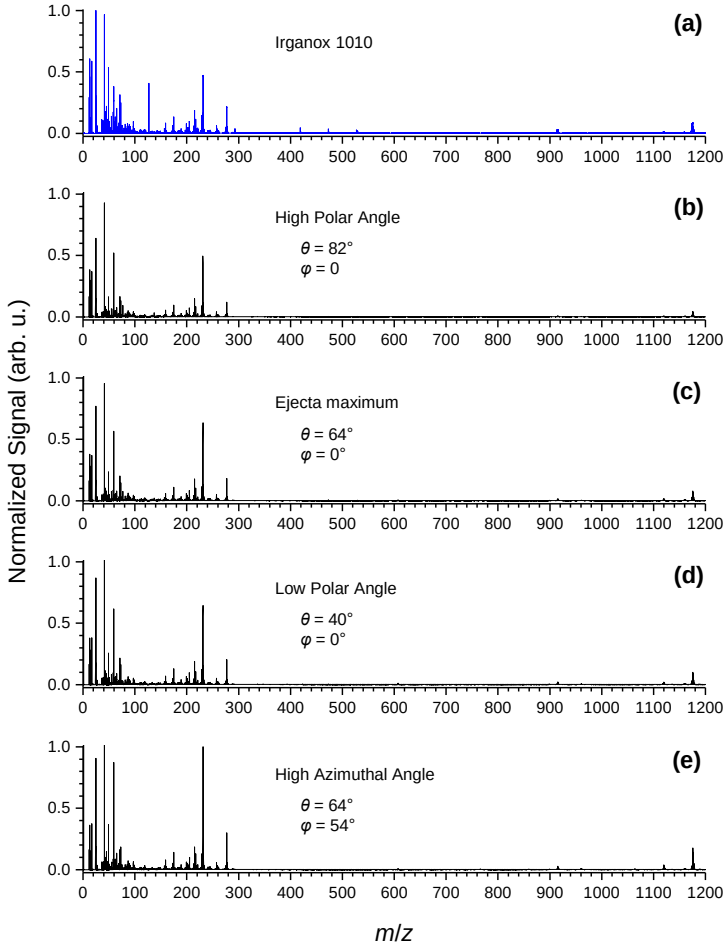

Figure SI-4. Change of SIMS spectra across a wide range of polar (b,c,d) and azimuthal (c,e) angles of ejection, in comparison to the SIMS spectrum for Irganox 1010 (a). The spectrum in panel (c) corresponds to the area in the thickness maps with the maximum deposit layer (cf. Figure SI-2a). Spectra were recorded in negative ion mode using a 25 keV Bi_3^+ analysis beam.

The spectra illustrate that no significant changes of the chemical composition of the collected material could be observed with increasing azimuthal and/or polar angles. Only minor shifts can be observed in the ratios of fragments. Most apparent is a signal gain with increasing azimuthal angle, which can be observed for molecular ion and fragments. This intensity gain might be the result of a changing contribution of matrix effects during the SIMS analysis on increasingly thinner layers of organic deposits toward the sides of the deposit.